RNAi-Mediated Allelic *trans*-Interaction at the Imprinted *Rtl1/Peg11* Locus

Erica Davis,[1] Florian Caiment,[1] Xavier Tordoir,[1]
Jérôme Cavaillé,[2] Anne Ferguson-Smith,[3]
Noelle Cockett,[4] Michel Georges,[1,*]
and Carole Charlier[1]
[1]Department of Genetics
Faculty of Veterinary Medicine
University of Liège
20 Boulevard de Colonster
4000 Liège
Belgium
[2]Laboratoire de Biologie Moléculaire Eucaryote
Centre National de la Recherche Scientifique
Unite Mixte de Recherche 5099
IFR-109
Université Paul Sabatier
31062 Toulouse
France
[3]Department of Anatomy
University of Cambridge
Cambridge CB2 3DY
United Kingdom
[4]Animal, Dairy, and Veterinary Sciences
College of Agriculture
Utah State University
Logan, Utah 84322-4700

Summary

The *Dlk1-Gtl2* imprinted domain, encompassing the callipyge (*CLPG*) locus in sheep, has recently been shown to harbor a large number of maternally expressed miRNA genes [1, 2]. Two of these (*mir127* and *mir136*) are processed from a transcript (*antiPeg11*) that is antisense to *Rtl1/Peg11*, a paternally expressed intronless gene with homology to the gag and pol polyproteins of Sushi-like retroelements [3]. We herein demonstrate that several additional miRNAs are processed from *antiPeg11* and that these regulate *Rtl1/Peg11* in *trans* by guiding RISC-mediated cleavage of its mRNA. This is the first demonstration of miRNA-mediated RNAi involving imprinted genes in mammals.

Results and Discussion

In Silico Prediction of Novel *(anti)Peg11*-Hosted miRNA Genes

We first aligned the human, mouse, rat, sheep, and dog *Rtl1/Peg11* gene sequences by using ClustalW. To improve the quality of the alignment, we performed a protein sequence alignment that we then back-translated into the respective nucleotide sequences. A cluster of tandem repeats (referred to as TRA, TRB, and TRC) at the 5′ end of *Rtl1/Peg11* was aligned manually (see Figures S1 and S2 in the Supplemental Data available with this article online).

*Correspondence: michel.georges@ulg.ac.be

We then generated a multispecies similarity profile by sliding an 80 bp window across the multiple alignment and by computing an average pair-wise identity score for each window. This allowed us to identify four hyperconserved regions of, respectively, 91 (region I), 124 (region II), 114 (region III), and 92 (region IV) bp, within which all 80 bp windows exhibited average pair-wise similarities of $\geq$ 98% (Figure 1). All four regions were shown to exhibit highly significant deficits in synonymous substitutions (see Supplemental Experimental Procedures), indicating that the corresponding gene segments undergo evolutionary constraints other than the protein sequence.

Hyperconserved regions III and IV coincide, respectively, with *mir127* and *mir136*, which are processed from the *antiPeg11* strand. To test whether hyperconserved regions I–IV might encode additional miRNA genes, we analyzed the corresponding sequences by using RNAfold [4]. As expected, conserved hairpin loops were detected on the *antiPeg11* strand for regions III and IV, corresponding to *mir127* and *mir136*. In addition, RNAfold also predicted conserved hairpin loops on the *antiPeg11* strand for regions I and II and on the *Rtl1/Peg11* strand for regions III and IV (but not I and II), suggesting that both *anti-Peg11* and *Rtl1/Peg11* might encode additional miRNA genes (Figure S3). The MiRscan scores [5] obtained with the human and mouse sequences for the corresponding RNA stem loops are shown in Figure 1.

By screening sequence databases, we identified a human miRNA (AY785934; hereafter referred to as *mir432*) mapping to the TRB tandem repetitions (*antiPeg11* strand). Its position coincides with a 90 bp window exhibiting an average pair-wise similarity of 95% when human, sheep, and dog sequences are compared. Analyzing the corresponding sequences by using RNAfold identified a strand-specific hairpin structure conserved in all three species (Figure S3) and yielded a MiRscan score (human-ovine) of 15.0 (Figure 1). We found no evidence for a stable hairpin loop in the corresponding rodent windows, which only exhibit an average pair-wise similarity of 62% with their human, ovine, and canine orthologs. However, when analyzing the rodent TRC repeats (which are absent in human, sheep, and dog), we identified conserved hairpins in both the *Rtl1/Peg11* and *antiPeg11* strands in a 94 bp window with 90% similarity between mouse and rat, and the resulting MiRscan scores (mouse – rat) were 4.2 and 13.2, respectively (Figure 1).

Hence, bioinformatic analysis predicts four *antiPeg11* miRNA precursors shared by all analyzed mammals in regions I–IV: one rodent-specific *antiPeg11* miRNA precursor in region TRC, one *antiPeg11* miRNA precursor shared by non-rodent mammals in region TRB, two *Rtl1/Peg11* miRNA precursors shared by all analyzed mammals in regions III and IV, and one rodent-specific *Rtl1/Peg11* miRNA precursor in region TRC.
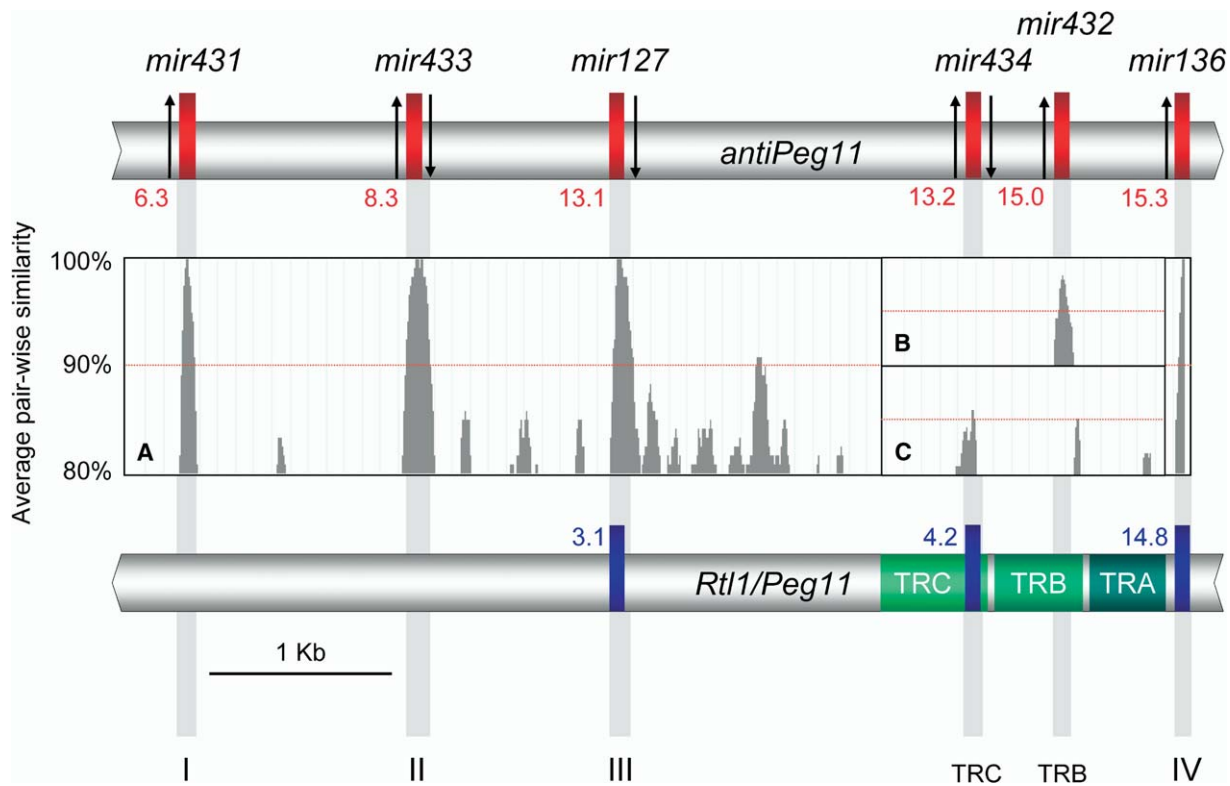
Figure 1. Bioinformatic Prediction of *(anti)Peg11*-Hosted miRNA Genes

Schematic representation of the *(anti)Peg11* locus showing (i) multispecies similarity profiles ([A] human, mouse, rat, sheep, and dog; [B] human, sheep, and dog; [C] mouse and rat) identifying four regions of extreme conservation (I, II, III, and IV) and two regions of high conservation (TRB and TRC), harboring evolutionarily conserved hairpin structures; (ii) pre-miRNAs predicted by MirScan (+ scores) in the conserved regions, highlighted in red when experimentally confirmed, in blue when not; (iii) arrows indicating from which arm the mature miRNAs are processed, and (iv) a cluster of tandem repeats (TRA, TRB, and TRC) highlighted as green boxes at the 5′ end of the *Rtl1/Peg11* open reading frame (See Figure S2).

Expression Analysis Confirms the *antiPeg11*- but Not *Rtl1/Peg11*-Hosted miRNAs

To verify which of these putative, in-silico-predicted, pre-miRNAs are processed into mature miRNAs, we performed primer extensions by using total RNA isolated from a range of murine tissues. We initially tested four to eight probes for each of the eight pre-miRNAs predicted in rodents (the TRB pre-miRNA was thus excluded); these probes targeted both stem-loop arms and were offset by 1–6 bp within a given arm (Table S1 in the Supplemental Data). As expected, we detected extension products for the 3′ arm of *mir127* and for the 5′ arm of *mir136*. In addition, we detected extension products corresponding to the 3′ arm of the *antiPeg11/* region I stem loop (hereafter referred to as *mir431*), for the 5′ and 3′ arms of the *antiPeg11*/region II stem loop (hereafter referred to as *mir433-5p* and *mir433-3p*), and for the 5′ and 3′ arms of the *antiPeg11*/TRC repeat stem loop (hereafter referred to as *mir434-5p* and *mir434-3p*). The specificity of the extension products was supported by the fact that each mature miRNA was detected by at least two probes yielding products of sizes compatible with the offset of the corresponding primers (Table S1 and Figure S4). We were not able to detect extension products for either of the pre-miRNAs pre-

dicted in the sense *Rtl1/Peg11* transcript, indicating that miRNAs are exclusively processed from *antiPeg11*.

All detected miRNA shared an expression profile similar to that of *Rtl1/Peg11*, i.e., preferentially expressed in embryo, placenta, brain, and skeletal muscle (Table S2) (Figure 2A). *mir127* and *mir136* were previously shown to be imprinted and preferentially expressed from the maternal allele; they were indeed detected in tissue samples from mUPD12 but not pUPD12 mice [1]. The same was demonstrated in this work for *mir431* (data not shown).

AntiPeg11-Hosted miRNAs Guide RISC-Mediated Cleavage of *Rtl1/Peg11* in vivo

We then tested whether *Rtl1/Peg11* is indeed a target for the detected *antiPeg11*-hosted miRNAs in vivo. To that end, we used mouse placental total RNA to perform RNA-ligase-mediated (RLM) 5′ RACE experiments [6] aimed at isolating the predicted RISC (RNA-induced silencing complex [7])-mediated *Rtl1/Peg11* mRNA cleavage products (Table S3).

One round of RT-PCR was sufficient to obtain clean RLM 5′ RACE products corresponding to regions I, III, TRC (two bands), and IV. The products of regions I, III, and IV and the largest band of region TRC were directly
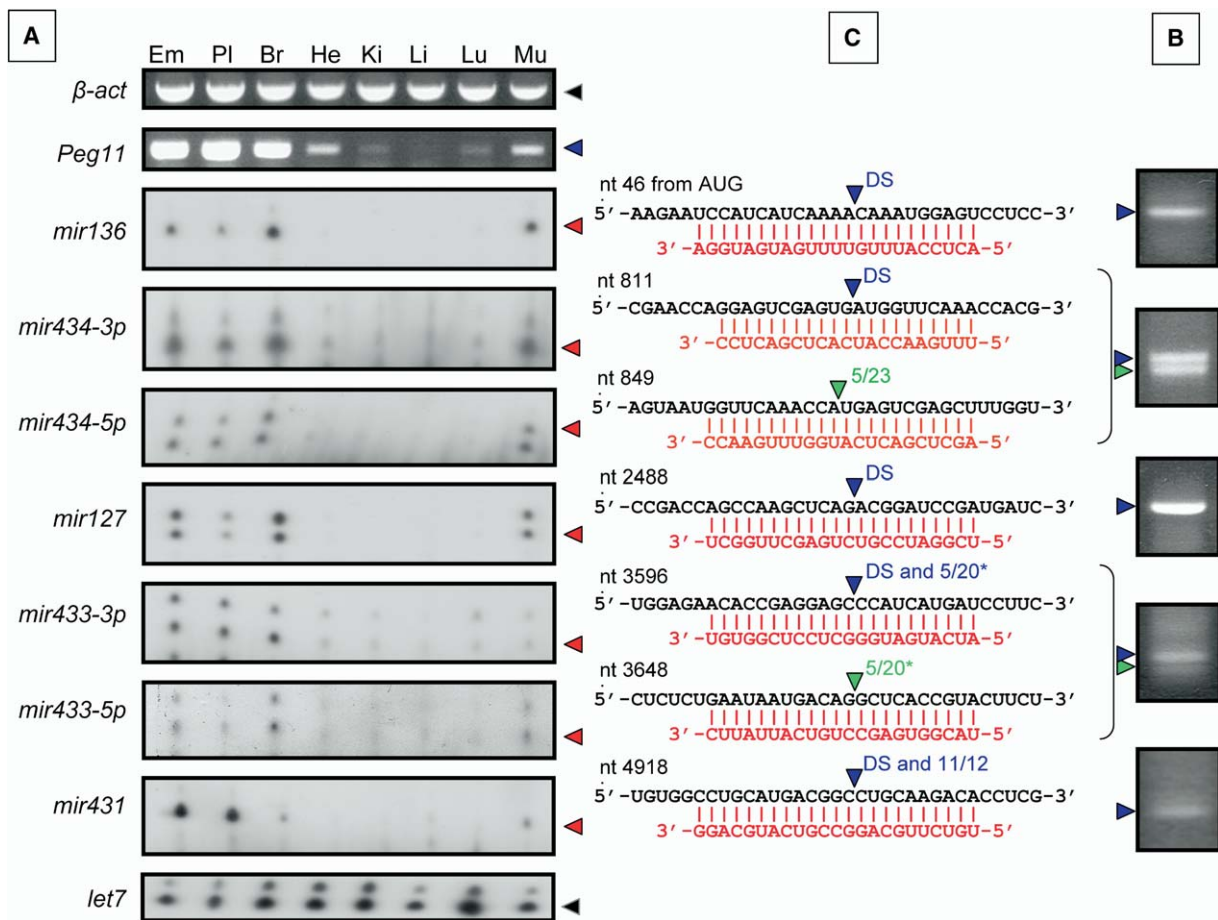
Figure 2. Detection of Mature *antiPeg11* miRNAs and Their Corresponding *Peg11* Cleavage Products

(A) Pre- (embryo [Em], placenta [Pl]) and post-natal (brain [Br], heart [He], kidney [Ki], liver [Li], lung [Lu], and skeletal muscle [Mu]) expression profile for *Rtl1/Peg11* and *β-actin* (RT-PCR), as well as *let7* and the seven *antiPeg11* miRNAs (primer extension).

(B) *Rtl1/Peg11* RLM 5′ RACE products identifying cleavage products directed by all seven *antiPeg11* miRNAs.

(C) Sequences of the seven *antiPeg11* miRNAs (red) hybridized to their respective *Rtl1/Peg11* targets (black); the arrows correspond to the cleavage sites identified by RLM 5′ RACE either by direct sequencing of the PCR products (DS) or by sequencing of individual cloned products (numbers indicate the fraction of clones that identify the predicted cleavage site; both *mirxa* PCR products were cloned jointly [*]).

sequenced and shown to correspond to *Rtl1/Peg11* mRNA cleavage products ending, as expected, at the nucleotide complementary to the 10th position of the respective mature miRNAs (*mir431, mir127, mir136,* and *mir434-3p*). The smaller TRC product was cloned, and the insert of 23 random clones was sequenced. Five of these were shown to correspond to the *Rtl1/Peg11* cleavage product expected for *mir434-5p*, ending in this case at the nucleotide complementary to the 11th position of this miRNA. The remaining clones correspond presumably to random *Rtl1/Peg11* degradation products. A second round of nested PCR was necessary to obtain two distinct bands corresponding to region II. These were cloned together, and the sequence of 20 randomly picked clones was determined. Five of these corresponded to the expected *mir433-5p*-guided *Rtl1/Peg11* cleavage products, five others to the expected *mir433-3p*-guided cleavage products. All ended at the nucleotide complementary to the 10th position of the respective mature miRNAs. The remaining

ten clones corresponded to distinct, presumably random *Rtl1/Peg11* degradation products. (Figures 2B and 2C).

These results unambiguously demonstrate the in vivo *trans*-inhibition of the paternally expressed *Rtl1/Peg11* by miRNAs processed from the maternally expressed *antiPeg11* precursor. They also demonstrate that *mir434* and *mir433* are unusual in that both stem-loop arms of the corresponding pre-miRNAs generate a mature miRNA incorporated in RISC.

The in vivo demonstration of *antiPeg11*-miRNA-mediated degradation of *Rtl1/Peg11* satisfactorily accounts for the previously reported observation of a 4- rather than 2-fold increase in *Rtl1/Peg11* mRNA levels in mice inheriting a deletion of the *Dlk1-Gtl2* imprinting control element (Δ-IGDMR) on their maternal chromosome. Such mice inherit two chromosomes with a paternal epigenotype and are thus expected to show a 2-fold increase in the expression levels of the paternally expressed protein-encoding genes, including *Rtl1/*
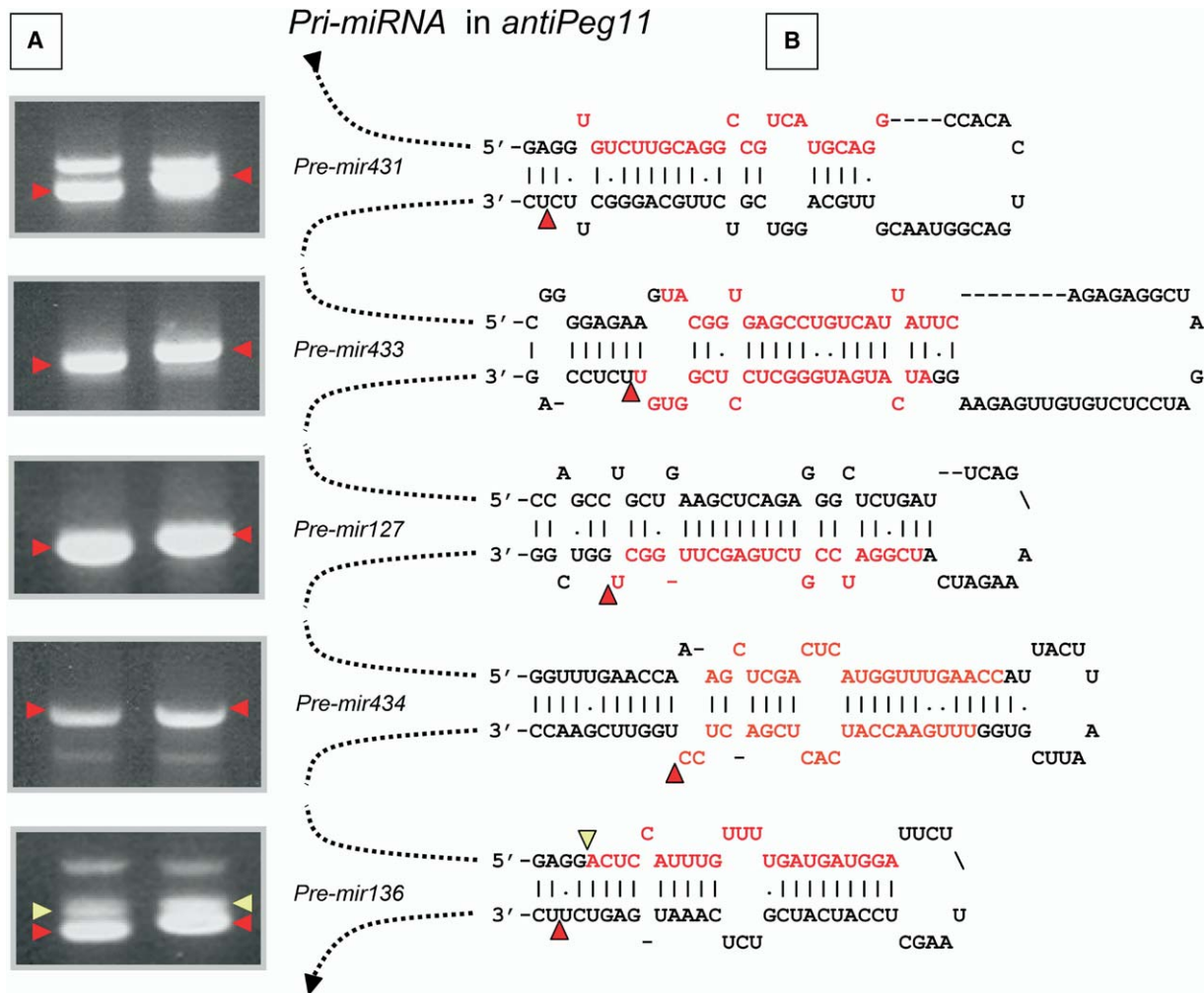
Figure 3. RLM 5′ RACE Experiments Targeting *antiPeg11* Identify Putative Drosha-Catalyzed Cleavage Products

(A) Agarose gel electrophoresis of the RLM 5′ RACE products targeting the four hyperconserved regions as well as the TRC region on the *antiPeg11* strand. The two lanes correspond to RACE products obtained with two distinct primer sets per region (see Table S3).

(B) Schematic representation of the five *antiPeg11* pre-miRNA stem loops highlighting the experimentally identified Drosha cleavage sites (arrows) and the mature miRNAs (in red).

Peg11. Our results indicate that the observed 4-fold increase is indeed due to the absence of the maternally expressed noncoding RNA genes, including the *antiPeg11*-miRNAs, and thus to the lack of RNAi-mediated *Rtl1/Peg11* degradation—as initially surmised [8].

Identification of Drosha Cleavage Products of *antiPeg11*-Hosted pri-miRNAs

We then applied the same RLM 5′ RACE technique, with murine placental RNA, to the *antiPeg11* strand in order to detect putative cleavage products that were mediated by mature miRNAs processed from the *Rtl1/Peg11* strand and that might not have been detected by primer extension. We initially selected primers to explore hyperconserved regions III and IV (Table S3). Strong RACE products were obtained in one round of RT-PCR and directly sequenced. They where shown to correspond to cleavage sites that mapped at the base

of the *mir127* and *mir136 antiPeg11* stem loops (3′ arm) at positions agreeing perfectly with those expected from the action of Drosha, the nuclear RNase III endonuclease that catalyzes pri-miRNA processing [7] (Figure 3).

We thus designed primers allowing us to scan the entire *antiPeg11* strand by RLM 5′ RACE (Table S3). Using the same procedure, we readily detected Drosha cleavage products corresponding to 3′ extremity of the *mir434*, *mir435*, and *mir431* stem loops. We also detected a cleavage product ending at the 5′ extremity of the *mir136* stem loop (and thus not cleaved at the 3′ extremity) and supposedly corresponding to an abundant processing intermediate. There was no evidence for Drosha processing of any other, as-yet-undetermined *antiPeg11* miRNA precursor, even in the TRB region (Figure 3).

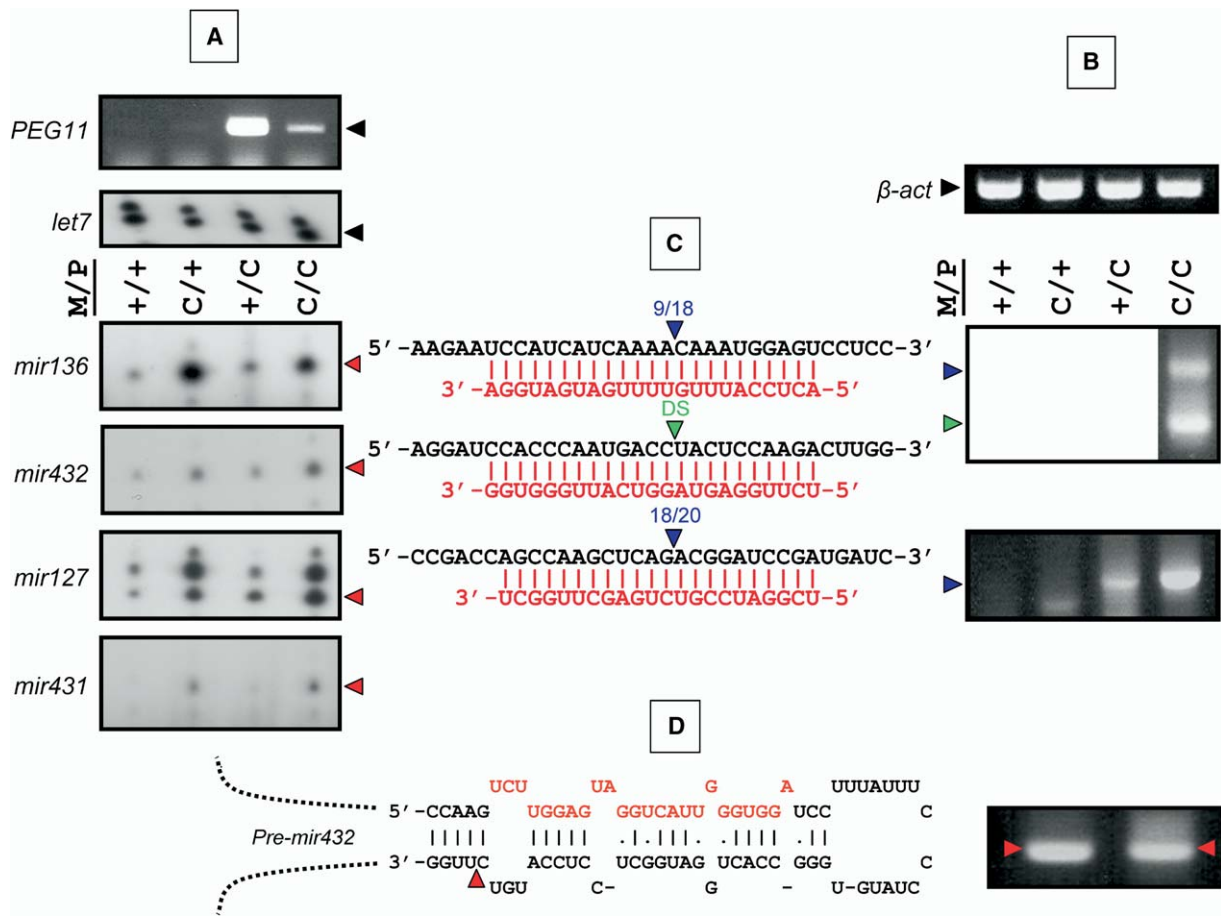These results thus provide additional independent

Figure 4. *antiPEG11*-miRNA and *PEG11* Expression, RISC-Mediated *PEG11* Cleavage, and Drosha Catalyzed Pre-*mir432* Processing in Ovine Skeletal Muscle

(A) Detection, in ovine longissimus dorsi, of mature *let7*, *mir136*, *mir432*, *mir127*, *mir431* (primer extension), and *PEG11* (RT-PCR; Table S2), showing the *cis* effect of the *CLPG* mutation on expression levels.

(B) RLM 5′ RACE products targeting intact *β-actin* as well as *mir136*, *mir432*, and *mir127*-guided cleavage products in ovine skeletal muscle.

(C) Sequences of *antiPEG11* miRNAs (red) hybridized to their *PEG11* target (black); the arrows correspond to the cleavage sites identified by RLM 5′ RACE either by direct sequencing of the PCR product (DS) or by sequencing of individual cloned products (numbers indicate the fraction of clones that identify the predicted cleavage site).

(D) Agarose gel electrophoresis of the RLM 5′ RACE products targeting the TRB region on the *antiPEG11* strand. The two lanes correspond to RACE products obtained with two distinct primer sets (see Table S3). Schematic representation of the pre-*mir432* stem loop highlighting the experimentally identified Drosha cleavage site (arrow) and the mature *mir432* (in red).

confirmation of the genuine nature of the five *anti-Peg11*-hosted murine miRNA genes yet of the absence of functional *Rtl1/Peg11*-hosted miRNA genes.

RNAi-Mediated Allelic *trans*-Interaction and the Conflict Hypothesis of Parental Imprinting

The strong expression of *Rtl1/Peg11* in the placenta, as well as the most striking symptom associated with *Rtl1/Peg11* overexpression (placentomegaly [9]), suggest that *Rtl1/Peg11* promotes a placental supply of maternal nutrients, as do other paternally expressed imprinted genes, including *Igf2* [10]. In this regard, it is interesting that we were not able to identify the ortholog of *Rtl1/Peg11* in 5.7 genome equivalents of the Fugu genome, 6.6 genome equivalents of the chicken genome, and 7.2 genome equivalents of the opossum

genome, suggesting that *Rtl1/Peg11* is eutherian specific.

The identification of maternally expressed *trans*-inhibitors of *Rtl1/Peg11* reveals a striking resemblance with the *trans*-inhibition of Igf2 by the maternally expressed Igf2r (after binding of Igf2 to Igf2r at the cell surface, the ligand-receptor complex is internalized and targeted to lysosomes in which Igf2 is degraded [10]). It suggests that the same evolutionary forces at the heart of the parental-conflict theory [11] have recruited RNAi in regulating fetal growth by selecting for mutations that create strand-specific pre-miRNAs in *antiPeg11* while leaving Rtl1/Peg11 unaltered. The occurrence of multiple *antiPeg11* miRNAs suggests that they are individually incapable of fully counteracting Rtl1/Peg11. Preliminary evidence for an unusual similarity among the

miRNA precursors suggests that they might be paraloguous and provides a glimpse in how this multilayered blocking system might have evolved (data not shown).

RNAi-Mediated Allelic *trans*-Interaction and Polar Overdominance

Our findings are particularly intriguing in light of the unusual inheritance pattern of the callipyge phenotype ("polar overdominance") in which only heterozygous individuals inheriting the *CLPG* mutation from their father express the muscular hypertrophy [12]. We have previously hypothesized that polar overdominance might involve the *trans*-inhibition of paternally expressed protein-encoding genes by maternally expressed noncoding RNA genes, possibly miRNAs uncovered within the *DLK1-GTL2* domain [13, 14].

To test whether the predicted *trans* interaction occurs between *PEG11* and the *antiPEG11*-hosted miRNA genes in skeletal muscle of sheep, we first examined the expression of the *antiPEG11* miRNAs in this tissue by means of primer extension. *mir127*, *mir136*, *mir431*, and a miRNA corresponding to the 3′ arm of the *anti-Peg11*/TRB repeat stem loop (hereafter referred to as *mir432*) were detected in longissimus dorsi of 8-week-old sheep representing the four possible genotypes at the *CLPG* locus ($+^{Mat}/+^{Pat}$, $CLPG^{Mat}/+^{Pat}$, $+^{Mat}/CLPG^{Pat}$, $CLPG^{Mat}/CLPG^{Pat}$). The genuine nature of the newly identified *mir432* miRNA was confirmed by the use of offset primers (Figure S4) and by the identification of the corresponding 3′ Drosha cleavage product (Figure 4D). The expression levels of all these miRNAs were affected by the *CLPG* mutation as expected in light of the fact that they were most abundant in $CLPG^{Mat}/+^{Pat}$ and $CLPG^{Mat}/CLPG^{Pat}$ individuals sharing the *CLPG* mutation on their maternal chromosome (Figure 4A).

We then performed RLM 5′ RACE experiments to detect putative *PEG11* cleavage products. We first used RNA from $CLPG^{Mat}/CLPG^{Pat}$ animals. Indeed, as a result of the *cis* effect of the *CLPG* mutation, these animals are overexpressing both *PEG11* and the *antiPEG11*-hosted miRNAs, and therefore cleavage products are predicted to be most abundant in $CLPG^{Mat}/CLPG^{Pat}$ individuals. Using a primer annealing downstream of the *mir127* complement, we obtained a band after two rounds of nested PCR. It was cloned, and the sequences of 18 out of 20 clones were shown to correspond to the expected *mir127*-mediated *PEG11* cleavage product. Using a primer annealing downstream of the *mir432* complement, we obtained two RACE products after two rounds of nested PCR. The smallest one was directly sequenced and shown to correspond to the expected *mir432*-mediated *PEG11* cleavage product. The larger one was cloned, and the sequences of nine out of 18 clones were shown to correspond to the expected *mir136*-mediated *PEG11* cleavage product (Figures 4B and 4C). We then performed the same RLM 5′ RACE experiments by using RNA extracted from skeletal muscle of 8-week-old $+^{Mat}/CLPG^{Pat}$, $CLPG^{Mat}/+^{Pat}$ and $+^{Mat}/+^{Pat}$ animals. A weak *mir127* cleavage product was obtained in $+^{Mat}/CLPG^{Pat}$ animals but not in the two other genotypes (Figure 4B). Neither *mir432* nor *mir136* cleavage products were detected in any of these animals (data not shown). The higher abundance

of the RACE products in $CLPG^{Mat}/CLPG^{Pat}$ animals when compared to the three other genotypes is thus in agreement with the known *cis* effect of the *CLPG* mutation. The miRNA-mediated degradation of *PEG11* transcripts in $CLPG^{Mat}/CLPG^{Pat}$ animals also satisfactorily explains why the *PEG11* RNA levels were systematically found to be lower in these animals when compared to $+^{Mat}/CLPG^{Pat}$ individuals (Figure 4A and [15]).

We are presently examining whether ectopic expression of *PEG11* might contribute to the induction of the callipyge phenotype and whether miRNA-mediated repression is involved in the previously reported *trans*-inhibition of DLK1, whose ectopic expression was shown to cause a callipyge-like phenotype in transgenic mice [16].

References

1. Seitz, H., Youngson, N., Lin, S.P., Dalbert, S., Paulsen, M., Bachellerie, J.P., Ferguson-Smith, A.C., and Cavaille, J. (2003). Imprinted microRNA genes transcribed antisense to a reciprocally imprinted retrotransposon-like gene. Nat. Genet. *34*, 261–262.

2. Seitz, H., Royo, H., Bortolin, M.L., Lin, S.P., Ferguson-Smith, A.C., and Cavaille, J. (2004). A large imprinted microRNA gene cluster at the mouse Dlk1-Gtl2 domain. Genome Res. *14*, 1741–1748.

3. Youngson, N., Kocialkowski, S., Peel, N., and Ferguson-Smith, A.C. (2005). A small family of sushi-class retrotransposon-derived genes in mammals and their relation to genomic imprinting. J. Mol. Evol., in press.

4. Hofacker, I.L., Fontana, W., Stadler, P.F., Bonhoeffer, S., Tacker, M., and Schuster, P. (1994). Fast folding and comparison of RNA secondary structures. Monatshefte f. Chemie *125*, 167–188.

5. Lim, L.P., Lau, N.C., Weinstein, E.G., Abdelhakim, A., Yekta, S., Rhoades, M.W., Burge, C.B., and Bartel, D.P. (2003). The microRNAs of Caenorhabditis elegans. Genes Dev. *17*, 991–1008.

6. Yekta, S., Shih, I.H., and Bartel, D.P. (2004). MicroRNA-directed cleavage of HOXB8 mRNA. Science *304*, 594–596.

7. Bartel, D.P. (2004). MicroRNAs: genomics, biogenesis, mechanism, and function. Cell *116*, 281–297.

8. Lin, S.P., Youngson, N., Takada, S., Seitz, H., Reik, W., Paulsen, M., Cavaille, J., and Ferguson-Smith, A.C. (2003). Asymmetric regulation of imprinting on the maternal and paternal chromo-

somes at the Dlk1-Gtl2 imprinted cluster on mouse chromosome 12. Nat. Genet. *35*, 97–102.

9. Georgiades, P., Watkins, M., Surani, M.A., and Ferguson-Smith, A.C. (2000). Parental origin-specific developmental defects in mice with uniparental disomy for chromosome 12. Development *127*, 4719–4728.

10. Reik, W., Constancia, M., Fowden, A., Anderson, N., Dean, W., Ferguson-Smith, A., Tycko, B., and Sibley, C. (2003). Regulation of supply and demand for maternal nutrients in mammals by imprinted genes. J. Physiol. *547*, 35–44.

11. Wilkins, J.F., and Haig, D. (2003). What good is genomic imprinting: the function of parent-specific gene expression. Nat. Rev. Genet. *4*, 1–10.

12. Cockett, N.E., Jackson, S.P., Shay, T.L., Farnir, F., Berghmans, S., Snowder, G.D., Nielsen, D.M., and Georges, M. (1996). Polar overdominance at the ovine callipyge locus. Science *273*, 236–238.

13. Georges, M., Charlier, C., and Cockett, N. (2003). The callipyge locus: evidence for the trans interaction of reciprocally imprinted genes. Trends Genet. *19*, 248–252.

14. Georges, M., Charlier, C., Smit, M., Davis, E., Shay, T., Tordoir, X., Takeda, H., Caiman, F., and Cockett, N. (2004). Toward molecular understanding of polar overdominance at the ovine callipyge locus. In Cold Spring Harbor Symposium on Quantitative Biology, B. Stillman and D. Stewart, eds. (Cold Spring Harbor, NY: Cold Spring Harbor Laboratory).

15. Charlier, C., Segers, K., Karim, L., Shay, T., Gyapay, G., Cockett, N., and Georges, M. (2001). The callipyge (CLPG) mutation enhances the expression of the coregulated *DLK1, GTL2, PEG11* and *MEG8* genes in *cis* without affecting their imprinting status. Nat. Genet. *27*, 367–369.

16. Davis, E., Harken Jensen, C., Schroder, H.D., Shay, T., Kliem, A., Cockett, N., Georges, M., and Charlier, C. (2004). Ectopic expression of DLK1 protein in skeletal muscle of padumnal heterozygotes causes the callipyge phenotype. Curr. Biol. *14*, 1858–1862.